Available online at www.sciencedirect.com
ScienceDirect
Mendeleev Commun., 2011, **21**, 250–252
Mendeleev Communications

Extremely short halogen bond: the nature and energy of iodine–oxygen interactions in crystalline iodic acid

Yulia V. Nelyubina, Mikhail Yu. Antipin and Konstantin A. Lyssenko*

A. N. Nesmeyanov Institute of Organoelement Compounds, Russian Academy of Sciences, 119991 Moscow, Russian Federation. Fax: +7 499 135 5085; e-mail: kostya@xrlab.ineos.ac.ru

DOI: 10.1016/j.mencom.2011.09.006

The mechanism of the hypercoordination of the iodine atom and its role in the crystal packing of iodic acid were examined within the topological analysis of the experimental electron density function.

If there is a tool in crystal engineering,[1–3] biochemistry and medicinal chemistry[4,5] as powerful as H-bonds, it is called halogen bonding, the term denoting the interaction between an electron donor and a covalently bound halogen atom.[2] Still gaining the popularity, the halogen bonding was the common subject of experimental and theoretical investigations[6,7] in the last decade. The theory describing its nature is now elaborated,[8–10] but its energy is analyzed mostly in the gas phase rather than in real solids,[11–14] the area of its application, although new methods to quantify its strength are being evolved. The topological analysis within Bader's Atoms in Molecule theory (AIM)[15] applied to the electron density distribution function in a crystal derived with the X-ray diffraction technique can be used to study the nature and to accurately estimate the strength[16,17] of halogen bonds in a real environment with other interactions (hydrogen bond, weak interactions, *etc*.) that can affect them.[18–23]

In this study, we have performed an X-ray diffraction (XRD)[†] investigation of the stable polymorph of iodic acid, α-HIO_3 (space group $P2_12_12_1$),[24,25] which features an extremely short I···O halogen bond [I···O 2.4830(10) Å, Figure 1] similar to that found in $La(IO_3)_3(HIO_3)$ [I···O 2.468(3) Å].[26] Besides this I···O interaction that most closely approaches the length of a single I–O bond [1.8984(10) Å] and thus can be considered a hypercoordinate bond, the crystal structure of α-HIO_3 contains four weaker I···O interactions [I···O 2.7362(10)–3.4441(10) Å] and an H-bond [O···O 2.6968(15) Å, OHO 168.1(10)°] involving the same oxygen atom as the hypercoordinate halogen bond does. In addition to performing a comparative analysis of different I···O interactions (which play an important role in stabilizing iodate compounds[27]), the presence of both hydrogen and halogen bonds makes HIO_3 a suitable system for assessing which of the two types of interactions is mainly responsible for cohesion in the crystal.

According to the XRD data for α-HIO_3, the I···O hypercoordination markedly distorts the geometry of the IO_3 moiety. This follows from the molecular and structural peculiarities of the metastable polymorphic modification of iodic acid, γ-HIO_3 (space group *Pbca*),[28] where the above hypercoordinate I···O bond is absent (Figure 1). In this case, the molecules are assembled by the analogous H-bond [O···O 2.665(2) Å], although leading to the formation of centrosymmetric dimers rather than H-bonded chains as in α-HIO_3, and four similar I···O interactions [I···O 2.689(2)–3.336(2) Å]. In three of these interactions, oxygens approach the iodine vertice of the IO_3 trigonal pyramid [the O···I–O angles with the opposite I–O bonds being 168.2(1)–174.3(1)°] in a way observed for the ClO_3^- anions in sodium chlorate [O–Cl···O 148.6(1)°];[29] the Cl···O interactions in the latter occurring as charge transfer from the oxygen lone pairs (LPs) to the σ* orbitals of the Cl–O bonds. In the crystal of γ-HIO_3, however, there is the additional interaction I(1)···O(1E) that involves the LP of the iodine atom [occupying the line passing through the I(1) atom and the centre of the O(1)O(2)O(3) triangle[29]]. Despite the similarity in the number and strength of the intermolecular contacts involving the iodine atom, the presence of the hypercoordinated I···O bond in the α-form of iodic acid causes the variations in its first coordination sphere [the same O···I–O angles are 132.85(5)–166.85(5)°]; hence, the mechanism of other I···O interactions therein may be different.

To get more insight into this hypercoordination and to evaluate the role of halogen and hydrogen bonds in the crystal packing formation, we have undertaken the topological analysis of the electron density distribution $\rho(r)$ in the crystal of α-HIO_3. According to its results, all the expected interactions (plus a couple of extra contacts, see Table 1) display the critical points (3,–1) or bond critical points (BCPs) in the corresponding interatomic areas of $\rho(r)$, which is the criterion for their bonding nature after the Bader's AIM theory.[15] Using the AIM notation,[15] the I–O bonds

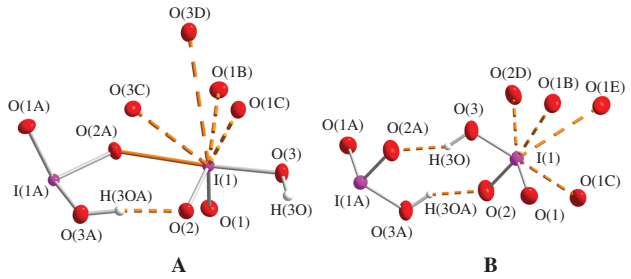

Figure 1 The general view of α-HIO_3 (**A**, current work) and γ-HIO_3 (**B**[28]) in the representation of atoms by thermal ellipsoids at p = 80%. The interatomic distances (Å) and angles (°) in α-HIO_3 are: I(1)–O(1) 1.7865(10), I(1)–O(2) 1.8147(10), I(1)–O(3) 1.8984(10), I(1)···O(2A) 2.4830(10), I(1)···O(1B) 2.7362(10), I(1)···O(1C) 2.8503(10), I(1)···O(3C) 3.3293(10), I(1)···O(3D) 3.4441(10), O(2)···O(3A) 2.6968(15); O(1)–I(1)–O(2) 100.64(5), O(1)–I(1)–O(3) 93.47(5), O(2)–I(1)–O(3) 97.50(4), O(3)–I(1)–O(2A) 174.46(4). The interatomic distances (Å) and angles (°) in γ-HIO_3 are:[28] I(1)–O(1) 1.804(2), I(1)–O(2) 1.911(2), I(1)–O(3) 1.873(2), I(1)···O(1B) 2.689(2), I(1)···O(1C) 2.694(2), I(1)···O(2D) 2.753(2), I(1)···O(1E) 3.336(2), O(2)···O(3A) 2.665(2); O(1)–I(1)–O(2) 101.3(1), O(1)–I(1)–O(3) 100.1(1), O(2)–I(1)–O(3) 96.4(1).

[†] Details of the X-ray diffraction data collection, the conventional (R = = 0.0155) and multipole (R = 0.0110) refinement, the topological analysis of the electron density function in the crystal of α-HIO_3 ($P2_12_12_1$, Z = 4) and the quantum chemical calculations can be found in Online Supplementary Materials. CSD 422563 contains the supporting crystallographic data for this paper. These data can be obtained free of charge from Fachinformationszentrum Karlsruhe, 76344 Eggenstein-Leopoldshafen, Germany (e-mail: crysdata@fiz-karlsruhe.de).

Table 1 Interatomic distances and topological parameters of $\rho(r)$ distribution in BCP of all the chemical bonds and intermolecular interactions in α-HIO_3.

Interaction[a]	R/Å	$\rho(r)$/ eÅ^{-3}	$\nabla^2\rho(r)$/ eÅ^{-5}	$-v(r)$/ a.u.	$h_e(r)$/ a.u.	E_{int}/ kcal mol^{-1}
I(1)–O(1)	1.7865(10)	1.84	–6.26	0.63709	–0.351	-
I(1)–O(2)	1.8147(10)	1.68	–0.32	0.56328	–0.283	-
I(1)–O(3)	1.8984(10)	1.52	–3.72	0.46485	–0.252	-
I(1)···O(2A)	2.4830(10)	0.37	3.08	0.05582	–0.012	17.5
O(2)···H(3OA)[b]	2.6968(15) [2.674]	0.28 [0.32]	5.32 [3.23]	0.04632 [0.0440]	0.0045 [–0.005]	14.5 [13.8]
I(1)···O(1B)	2.7362(10) [2.673]	0.18 [0.22]	1.79 [2.04]	0.02040 [0.0216]	0.001 [–0.0002]	6.4 [6.8]
I(1)···O(1C)	2.8503(10)	0.15	1.52	0.01505	0.001	4.7
I(1)···O(3C)	3.3293(10)	0.08	0.91	0.00667	0.001	2.1
I(1)···O(3D)	3.4441(10)	0.07	0.86	0.00561	0.002	1.8
O(1)···O(3E)	3.0661(15)	0.05	0.71	0.00403	0.002	1.3
O(3)···O(3E)	3.0898(15)	0.05	0.67	0.00371	0.002	1.2

[a]The symmetry-generated atoms are obtained from the basic ones by symmetry operations: O(2A) and H(3OA) by $-x$, $y+0.5$, $-z+0.5$; O(1B) by $x+0.5$, $-y+0.5$, $-z$; O(1C) and O(3C) by $-x+0.5$, $-y$, $z+0.5$; O(3D) by $-x+1$, $y+0.5$, $-z+0.5$; O(3E) by $x-0.5$, $-y-0.5$, $-z$; the geometrical and topological parameters for the H-bond and the I···O interaction according to the DFT calculations are given in brackets. [b]The distance between the oxygen atoms involved in the H-bonding is given.

are classified as shared interactions, which are common for covalent bonds; the electron energy densities $h_e(r)$ at their BCPs are negative (Table 1) and those of $\nabla^2\rho(r)$ vary from –6.26 to –0.32 eÅ^{-5} (the significant variation of the latter values is a well-known feature of polar bonds and was discussed in detail earlier;[30] in this case, it is also due to the I–O lengths being different as a result of different interactions with the crystal environment).

The H-bond, as well as the secondary I(1)···O(1) and I(1)···O(3) interactions (together with the additional O···O binding[31]), in α-HIO_3 belongs to the closed-shell type with the positive values of both the $h_e(r)$ and $\nabla^2\rho(r)$ functions (Table 1). The hypercoordinate I···O(2A) bond is intermediate between these intermolecular interactions and the covalent I–O bonds [$\rho(r) = 0.37$ eÅ^{-3}, $\nabla^2\rho(r) = 3.08$ eÅ^{-5}, $h_e(r) = -0.012$ a.u.] with a significant covalent contribution supporting the hypervalent character of the iodine atom.[10] Note that the same intermediate type of bonding was observed earlier for the hypercoordinate bonds involving Si and Ge atoms.[32,33]

To determine the mechanism of the I···O hypercoordination (within the charge-transfer model[10]), we have constructed the 3D-distributions of the deformation electron density (DED) and the electron localization function (ELF),[34] which are used to visualize the areas of electron accumulation or depletion. The inspection of the two functions in α-HIO_3 (Figure 2 and Figure S1 in Online Supplementary Materials) revealed one diffuse LP domain of the I(1) atom significantly deviating from the position expected for the IO_3 moiety (see above).

Interacting with the oxygen atoms (each possessing three LPs) of the neighboring HIO_3 species, the iodine atom acts both as a donor and an acceptor of electron density. The iodine LP is directed towards the O(1C) atom [I···O 2.8503(10) Å], while the area of the electron density depletion near it coincides with the position of an LP of the O(2A) atom. Thus, the I(1)···O(2A) hypercoordination of the iodine clearly occurs *via* the charge transfer from this LP to the σ* orbital of the I(1)–O(3) bond and hereinafter is referenced as the O(2A)→I bond. The same direction of the charge transfer – LP(O)→σ*[I(1)–O(2)] – is observed for the O(1B) atom, whereas the I···O(1C) interaction is formed with the iodine LP as a donor. In the case of the weaker I···O(3) interactions [not shown, I···O 3.3293(10)–3.4441(10) Å], the charge is also transferred from the oxygen LP to the σ* orbital of the corresponding I–O bond.

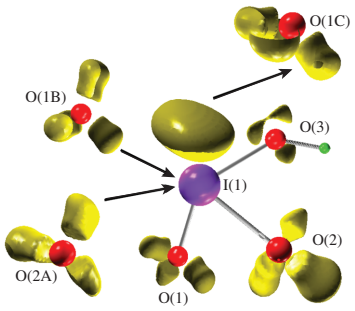

Figure 2 The 3D-distribution of ELF in the section of the I···O interactions in α-HIO_3. Isosurface with ELF = 0.8 is shown.

To further confirm the pathways of the charge transfer accompanying the I···O(2A) binding, we have performed the DFT calculation of the dimer of iodic acid assembled by the H-bond and the I···O interaction (Figure 3). The optimization of this moiety led to the geometric characteristics for the H-bond (O···O 2.674 Å) well reproducing those in the crystal, while the I···O interaction was significantly weakened in the gas phase [I···O 2.673 Å, O(2A)I(1)O(3) 166.2°]. As a result, the topological parameters in the BCP for the H-bond [$\rho(r) = 0.32$ eÅ^{-3}, $\nabla^2\rho(r) = 3.23$ eÅ^{-5}, $h_e(r) = -0.00520$ a.u.] in the isolated dimer are almost the same as in the crystal, while in the case of the O···I bonding [$\rho(r) = 0.22$ eÅ^{-3}, $\nabla^2\rho(r) = 2.04$ eÅ^{-5}, $h_e(r) = -0.00022$ a.u.] they are comparable with those for the I(1)···O(1B) interaction (Table 1) of the similar length.

The atomic charges (Figure 3 and Table S1 in the Online Supplementary Materials) obtained for the model dimer clearly indicate that the two types of bonding (the H-bond and the I···O interaction) are characterized by the analogous charge redistribution pattern, namely, by the increase in the electron population of the oxygen atoms involved [O(2), O(3A) and O(3), O(2A), respectively] and its decrease on the hydrogen H(3OA) and iodine I(1) atoms; the value for the latter being close to one in the crystal of α-HIO_3 (+2.20 e). Therefore, the mechanism of charge transfer for the O(2A)→I–O bond is the same as for other stereoelectronic interactions.[35] This also agrees with the molecular and structural peculiarities of the γ-modification of iodic acid, which lacks the above hypercoordinate O(2A)→I bond.[28] Given that the H-bond therein is as strong as in α-HIO_3, a small elongation of the I(1)–O(3)H bond from 1.873(2) Å in the former to 1.8984(10) Å in the latter is caused by the hypercoordinate I···O bond also confirming the O→I–O(H) charge transfer mechanism of its formation.

Note that, with the H-bond of the same strength and the I···O distances even shorter [if the O(2A)→I bonding is not considered], γ-HIO_3 is metastable. This allows us to conclude that the stability of the α-polymorph of HIO_3 is governed by this hypercoordinate O(2A)→I interaction rather than the H-bond. The latter is also supported by the fact that similar seesaw-like motif of supramolecular organization persists in the isoelectronic and isomorphous systems, IO_2F[36] and XeO_3[37] (although in these cases the additional O···F and O···O interactions, instead of the hydrogen

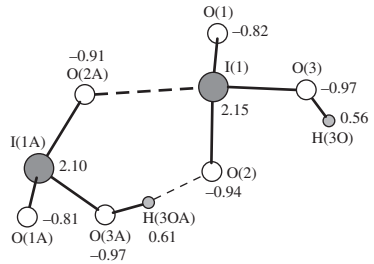

Figure 3 Optimized HIO_3 dimer formed by the H-bond and the I···O interaction showing the atomic charges according to the DFT calculations.

bond in α-HIO_3, can also contribute to their cohesion). To make a quantitative conclusion, the energy of all the interactions in a crystal of α-HIO_3 was estimated based on the proportionality between the energy of an interaction (E_{int}) and the potential electron density $v(r)$ in its BCP.[16,17] In line with the values obtained, the energy of the O(2A)→I interaction reaches 17.5 kcal mol^{-1}, that of the hydrogen bond is ~15 kcal mol^{-1} (Table 1). Such an energetic superiority of the O(2A)→I interaction in α-HIO_3 agrees with the fact that the iodine, in contrast to the lighter halogens for which the H-bonding is energetically favored,[7] is able to form the halogen bonds that are comparable or even stronger than the H-bonds.[2] Moreover, the other I···O interactions in this case contribute the same value of 15 kcal mol^{-1} as the H-bond does; the energy of all the interactions that enable the formation of the crystalline α-HIO_3 approaching 49.4 kcal mol^{-1}. The accuracy of the above estimates somewhat follows from the interaction energies for the above dimer $(HIO_3)_2$ calculated through the Espinosa correlation (Table 1); the corresponding values are close to those for the H-bond (calc. E_{int} = 13.8 kcal mol^{-1}) and the I(1)···O(1B) interaction (calc. E_{int} = 6.8 kcal mol^{-1}) in the crystal of α-HIO_3. For comparison, the I···O halogen bond of the similar length [2.7253(10) Å][20] in the complex of 4,4′-dipyridyl-*N*,*N*′-dioxide with 1,4-diiodotetrafluorobenzene has an energy of ~7.4 kcal mol^{-1}.

Independently, the relative strengths of these types of bonding can be assessed from the DFT data by comparing the atomic energies E_{at}[38] for the atoms that are involved in the H-bond or the halogen bond and those that form neither of them, the O(1) and O(1A) atoms in this case (Figure 3 and Table S1). The differences in the corresponding values for the O(2) and O(1) atoms and for their symmetry-related partners O(1A) and O(2A) attributed to the energetic changes due to the formation of the H-bond and the O···I interaction are 27.2 and 18.8 kcal mol^{-1}, respectively; the latter indicating that the H-bond is much stronger. The similar trend is observed for the differences in the E_{at} values for the atomic pairs O(2) and O(2A) (ΔE_{at} = 12.1 kcal mol^{-1}), O(3) and O(3A) (ΔE_{at} = 14.5 kcal mol^{-1}). In addition to the variations in the atomic energies, the halogen and hydrogen bonding causes the distinction between the molecular energies for the two HIO_3 species of the dimer by 6.9 kcal mol^{-1}, which corresponds to the transfer of 0.02 e between them; the latter agreeing with the experimental data reported earlier for the systems with several independent molecules.[39] All of the above E_{at}-based estimates qualitatively coincide with the Espinosa interaction energies and lead to the same conclusion about the hydrogen bonding being more energetically favorable in the gas phase than the halogen bonding is. In a condensed state, however, this relation might invert, as evidenced by the significant shortening of the O(2A)→I bond distance in the crystal of α-HIO_3.

Therefore, we may conclude that, in the case of HIO_3 the charge transfer O→I–O is the main source of the hypercoodination of the iodine atom; the latter being largely responsible for the stabilization of the α-polymorph of iodic acid. Although with the exception of the extremely short (hypercoordinate) halogen bonds, the I···O interactions are generally weaker than the H-bonds of the moderate strength, a bunch of them can easily become comparable with or even overcome the hydrogen bonding in contributing to the crystal packing formation. Moreover, taking into account how frequently the I···O interactions[27] occur in a solid state world, this is likely to be an inherent feature of the IO_3^- moiety.

This study was supported by the Russian Foundation for Basic Research (project nos. 10-03-00578 and 11-03-92697) and the Foundation of the President of the Russian Federation (Federal Programme for the Support of Young Doctors, grant MD-237.210.3).

Online Supplementary Materials

Supplementary data associated with this article can be found in the online version at doi:10.1016/j.mencom.2011.09.006.

References

1 P. Metrangolo and G. Resnati, *Chem. Eur. J.*, 2001, **7**, 2511.
2 P. Metrangolo, H. Neukirch, T. Pilati and G. Resnati, *Acc. Chem. Res.*, 2005, **38**, 386.
3 S. K. Ritter, *Chem. Eng. News*, 2009, **87**, 39.
4 L. A. Hardegger, B. Kuhn, B. Spinnler, L. Anselm, R. Ecabert, M. Stihle, B. Gsell, R. Thoma, J. Diez, J. Benz, J.-M. Plancher, G. Hartmann, D. W. Banner, W. Haap and F. Diederich, *Angew. Chem. Int. Ed.*, 2011, **50**, 314.
5 P. Auffinger, F. A. Hays, E. Westhof and P. Shing Ho, *PNAS*, 2004, **101**, 16789.
6 J. E. Del Bene, I. Alkorta and J. Elguero, *J. Phys. Chem. A*, 2010, **114**, 12958, and references therein.
7 I. Alkorta, F. Blanco, M. Solimannejad and J. Elguero, *J. Phys. Chem. A*, 2008, **112**, 10856, and references therein.
8 T. Clark, M. Hennemann, J. S. Murray and P. Politzer, *J. Mol. Model.*, 2007, **13**, 291.
9 T. T. T. Bui, S. Dahaoui, C. Lecomte, G. R. Desiraju and E. Espinosa, *Angew. Chem. Int. Ed.*, 2009, **121**, 3896.
10 M. C. Aragoni, M. Arca, F. A. Devillanova, A. Garau, F. Isaia, V. Lippolis and A. Mancini, *Bioinorg. Chem. Appl.*, 2007, **2007**, 14416.
11 N. J. Martinez-Amezaga, S. C. Pamies, N. M. Peruchena and G. L. Sosa, *J. Phys. Chem. A*, 2010, **114**, 552.
12 F. F. Awwadi, R. D. Willett and B. Twamly, *J. Mol. Struct.*, 2009, **918**, 116.
13 Y. H. Wang, Y. X. Lu, J. W. Zou and Q. S. Yu, *Int. J. Quant. Chem*., 2008, **108**, 90.
14 Y. X. Lu, J. W. Zou, Y. H. Wang and Q. S. Yu, *J. Mol. Struct. THEOCHEM*, 2006, **776**, 83.
15 R. F. W. Bader, *Atoms in Molecules. A Quantum Theory*, Clarendon Press, Oxford, 1990.
16 E. Espinosa, E. Molins and C. Lecomte, *Chem. Phys. Lett*., 1998, **285**, 170.
17 E. Espinosa, I. Alkorta, I. Rozas, J. Elguero and E. Molins, *Chem. Phys. Lett.*, 2001, **336**, 457.
18 Yu. V. Nelyubina, M. Yu. Antipin, D. S. Dunin, V. Y. Kotov and K. A. Lyssenko, *Chem. Commun.*, 2010, **46**, 5325.
19 V. R. Hathwar and T. N. G. Row, *J. Phys. Chem. A*, 2010, **114**, 13434.
20 R. Bianchi, A. Forni and T. Pilati, *Acta Crystallogr, Sect. B*, 2004, **60**, 559.
21 V. G. Tsirelson, P. F. Zou, T. H. Tang and R. F. W. Bader, *Acta Crystallogr., Sect. A*, 1995, **51**, 143.
22 R. Boese, A. D. Boese, D. Blaser, M. Y. Antipin, A. Ellern and K. Seppelt, *Angew. Chem., Int. Ed. Engl*., 1997, **36**, 1489.
23 A. V. Shishkina, A. I. Stash, B. Civalleri, A. Ellern and V. G. Tsirelson, *Mendeleev Commun*., 2010, **20**, 161.
24 M. T. Rogers and L. Helmholz, *J. Am. Chem. Soc.*, 1941, **63**, 278.
25 K. Stahl and M. Szafranski, *Acta Chem. Scand.*, 1992, **46**, 1146.
26 M. B. Taouti, A. Gacemi, D. Benbertal and I. Gautier-Luneau, *Z. Kristallogr.*, 2008, **223**, 179.
27 J. Ling and T. E. Albrecht-Schmitt, *Inorg. Chem*., 2007, **46**, 346.
28 A. Fischer and M. Lindsjo, *Z. Anorg. Allg. Chem.*, 2005, **631**, 1574.
29 Yu. V. Nelyubina, K. A. Lyssenko, R. G. Kostyanovsky, D. A. Bakulin and M. Yu. Antipin, *Mendeleev Commun*., 2008, **18**, 29.
30 J. Henn, D. Ilge, D. Leusser, D. Stalke and B. Engels, *J. Phys. Chem. A*, 2004, **108**, 9442.
31 Yu. V. Nelyubina, M. Yu. Antipin and K. A. Lyssenko, *Usp. Khim.*, 2010, **79**, 195 (*Russ. Chem. Rev.*, 2010, **79**, 167).
32 A. A. Korlyukov, K. A. Lyssenko, M. Y. Antipin, V. N. Kirin, E. A. Chernyshev and S. P. Knyazev, *Inorg. Chem*., 2002, **41**, 5043.
33 M. G. K. Voronkov, A. A. Korlyukov, E. A. Zelbst, S. P. Knyazev, I. M. Vasil'ev, E. A. Chernyshev and M. Y. Antipin, *J. Struct. Chem.*, 2010, **51**, 719.
34 V. Tsirelson and A. Stash, *Chem. Phys. Lett.*, 2002, **351**, 142.
35 I. S. Bushmarinov, M. Y. Antipin, V. R. Akhmetova, G. R. Nadyrgulova and K. A. Lyssenko, *J. Phys. Chem. A*, 2008, **112**, 5017.
36 R. Minkwitz, M. Berkei and R. Ludwig, *Inorg. Chem*., 2001, **40**, 6493.
37 D. H. Templeton, A. Zalkin, J. D. Forrester and S. W. Williamson, *J. Am. Chem. Soc*., 1963, **85**, 817.
38 I. S. Bushmarinov, K. A. Lyssenko and M. Yu. Antipin, *Usp. Khim.*, 2009, **78**, 307 (*Russ. Chem. Rev.*, 2009, **78**, 283).
39 Y. V. Nelyubina, M. Y. Antipin, I. A. Cherepanov and K. A. Lyssenko, *CrystEngComm*, 2010, **12**, 77.

Received: 21st January 2011; Com. 11/3668